Bulletin of the Seismological Society of America. Vol. 48, pp. 1–15. January 1958

Bulletin of the Seismological Society of America

Vol. 48 JANUARY, 1958 No. 1

THE AFTERSHOCK SEQUENCE OF THE KAMCHATKA EARTHQUAKE OF NOVEMBER 4, 1952

By MARKUS BÅTH and HUGO BENIOFF

ABSTRACT

Aftershock epicenters of the Kamchatka earthquake of November 4, 1952, are distributed over an area approximately 1,030 kilometers in length by 240 kilometers in width. Assuming that this distribution represents the active strain zone, the total average strain, average elastic energy, and average stress of the rocks before slip were 11.9×10^{-5}, 1.35×10^{2} ergs/cm.^{3}, and 12.6 kg/cm.^{2}, respectively.

The strain-release curve of the sequence has been constructed using observations from Uppsala and Kiruna. The data include more than 400 shocks with magnitudes 6.0 and greater which have occurred up to December, 1956. The curve exhibits three segments each of the form $\Sigma J^{\frac{1}{2}} = A + B \log t$, where J is the energy and t is the time measured from the time of the principal earthquake. The slope B changes abruptly at $t = 0.4$ days and at $t = 195$ days, the latter change being particularly pronounced. Moreover, this was accompanied by other evidence suggesting a change in mechanism. The coefficients B have almost the exact ratio of 1 : 2 : 5 in the three intervals 0–0.4, 0.4–195, and after 195 days. The aftershock activity has its highest concentration in the vicinity of the principal earthquake and tapers off toward both ends of the active fault segment. The majority of the aftershocks have clear pP impulses occurring generally 9 to 13 sec. after P, indicating that the foci were in or close to the Mohorovičić discontinuity. The rate of strain accumulation and release for the time interval from 1897 to 1956 for the entire Kamchatka–northern Japan stress system shows a slow decrease with time. Comparison of the rate of the entire system with that of the aftershock sequence leads to an approximate estimate of the possible duration of the sequence.

1. OBSERVATIONAL DATA AND METHODS

THE occurrence on November 4, 1952, at 16:58:26 G.M.T. of an 8.5 magnitude earthquake off the east coast of Kamchatka ($\lambda = 159\frac{1}{2}°$ E, $\phi = 52\frac{3}{4}°$ N) provided an opportunity for investigating the aftershock sequence strain-release characteristic of a great earthquake. Heretofore aftershock release studies have been limited to shocks of magnitudes 7.7 or less (Benioff, 1951*a*, 1955*a*, *b*). The Kamchatka sequence exhibits several new features not observed earlier.

Records of the seismograph stations at Uppsala and Kiruna, especially those written with the short-period vertical instruments, have provided a homogeneous material, from which the strain-release curve has been constructed. The original observational data can be found in the Uppsala and Kiruna seismological bulletins. They contain a much more complete listing of the Kamchatka aftershocks than any other available bulletin. The magnitudes M were determined on the basis of the original scale for every shock in which the observed ground amplitude of P was equal

Manuscript received for publication March 14, 1957.

to or greater than 0.05 microns. In the annual bulletins for 1954 and earlier, station corrections etc. were not applied, which, however, was done for this study. The magnitudes determined from the records of the two stations do not differ in general by more than one-fourth of a unit. Mean values of the Kiruna and Uppsala magnitudes were used, which agree with determinations from other station records within approximately one-fourth of a magnitude. It often happened that surface waves could not be used for magnitude determinations, since most of the aftershocks occurred at somewhat greater depth than normal.

In calculating a quantity proportional to the strain the method used earlier (Benioff, 1951*a*, pp. 41–42) was applied. In order to bring forward a slight refinement of the method, a modified derivation is given here. We use the following notation:

W = potential strain energy per unit volume
J = seismic wave energy
V = total volume of strained rock
k = incompressibility
μ = rigidity
p = fraction of potential strain energy converted into seismic wave energy
θ ($= e_{ii}$) and e_{ij} = strain (for expressions see Bullen, 1947).

Indices c and s refer to compression and shear respectively, no index indicates the total values. We then have the following relations

$$J_c = p_c W_c V_c = p_c \frac{k}{2} \theta^2 V_c \tag{1}$$

$$J_s = p_s W_s V_s = p_s \mu \left(e_{ij}^2 - \frac{1}{3} \theta^2 \right) V_s \tag{2}$$

$$J = J_c + J_s \tag{3}$$

According to Bullen (1947, p. 220), we have for a depth of 33 km., where most of the aftershocks occurred (see below), $k/2 = 0.58 \times 10^{12}$ dynes/cm.^{2} and $\mu = 0.63 \times 10^{12}$ dynes/cm.^{2}, and therefore $k/2 \simeq \mu \equiv \bar{\mu}$. In the absence of contrary information we assume that $p_c = p_s \equiv p$ and that $V_c = V_s \equiv V$, the latter assumption being particularly uncertain. This gives us

$$J = J_c + J_s = p\bar{\mu}\left(e_{ij}^2 + \frac{2}{3} \theta^2 \right) V = \frac{1}{2} p\bar{\mu}\epsilon^2 V \tag{4}$$

or

$$J^{\frac{1}{2}} = \left(\frac{1}{2} p\bar{\mu} V \right)^{\frac{1}{2}} \epsilon = c\epsilon \tag{5}$$

where

$$\epsilon = \left(2e_{ij}^2 + \frac{4}{3} \theta^2 \right)^{\frac{1}{2}} \tag{6}$$

and c is a constant for a given fault system. For a sequence of aftershocks the strain ϵ is given by

$$\Sigma\epsilon = \frac{1}{c} \Sigma J^{\frac{1}{2}} \tag{7}$$

Since c is unknown and is a constant, it is sufficient for our purpose to plot $\Sigma J^{\frac{1}{2}}$. Unfortunately, the present status of seismology is not sufficiently advanced to make effective use of the refinement given here.

The energy J (ergs) has been computed from the magnitude M from the formula

$$\log_{10} J = 9 + 1.8\,M \tag{8}$$

or

$$\log_{10} J^{\frac{1}{2}} = 4.5 + 0.9\,M \tag{8^1}$$

(see Benioff, 1955*a*, *b*). The relation between J and M has recently been subjected to several revisions, but for the present purpose, where we are much more concerned with time variations of $\Sigma J^{\frac{1}{2}}$ than with its absolute values, we use the formula given above, which also facilitates comparison with earlier sequences (Benioff, 1955*a*, *b*). Considering the inevitable errors in the M determination, the differences are not important, since in the latest formula of Gutenberg and Richter (1956) for $J^{\frac{1}{2}}$ the coefficient of M is 0.75 instead of 0.9.

Combining the formula for J given above with the expression of M for a P wave with vertical amplitude u microns and period t sec., we may write

$$J^{\frac{1}{2}} = \alpha \frac{u}{t} \tag{9}$$

where α is a constant for a given station, and

$$\Sigma\epsilon = \frac{\alpha}{c}\,\Sigma\,\frac{u}{t} \tag{10}$$

If the vertical component of the P wave at a given station is used consistently, $\Sigma(u/t)$ will represent the strain release without the necessity of computing the magnitude. The formula may also be more generally applied, remembering that α varies with the epicentral distance, the focal depth, the kind of wave used, and the component, and that it also includes station corrections. In this paper, however, we are using the magnitudes.

In order to obtain a maximum homogeneity the material was limited as follows:

a) *Geographical distribution.*—A plot on a map of all shocks occurring since November 4, 1952, in Kamchatka and the Kurile Islands for which locations were given by USCGS or BCIS, shows that the aftershock area is well defined in all directions. The area is shown in figure 1. Even the southern limit at 47°–48° N coincides with other features, marked both by a gap in the earthquake belt and a change in its direction. The aftershock area includes therefore Kamchatka and the northern Kurile Islands. It is 1,030 km. long by 240 km. wide. We assume that this area represents the extent of the stress system, which generated both the principal earthquake and the aftershock sequence. On the basis of evidence from the Kern County, California, earthquake of 1952 (Benioff, 1955*a*, *b*) it can be assumed further that during the principal earthquake faulting extended approximately the entire length of the area.

The map (fig. 1) shows all aftershocks for which accurate epicentral locations are known. The total aftershock strain release represented by these shocks for each of the lettered transverse areas is plotted in figure 2. This figure shows that the after-

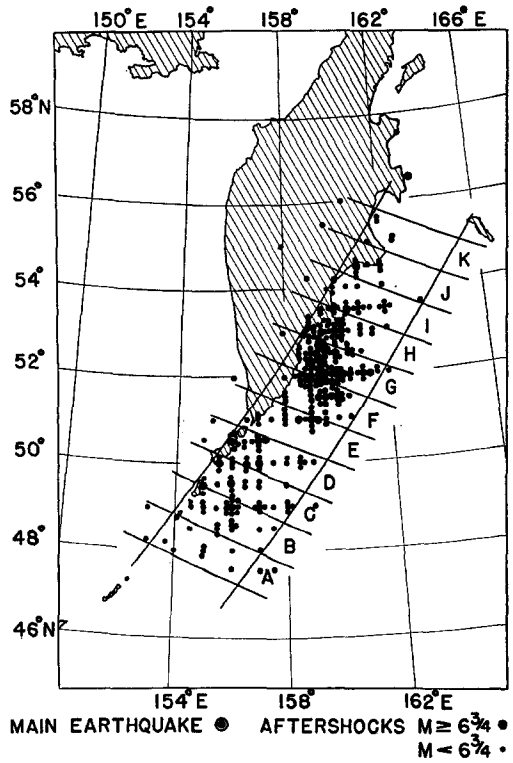

Fig. 1. Map showing aftershock area and all aftershocks for which accurate locations were known.

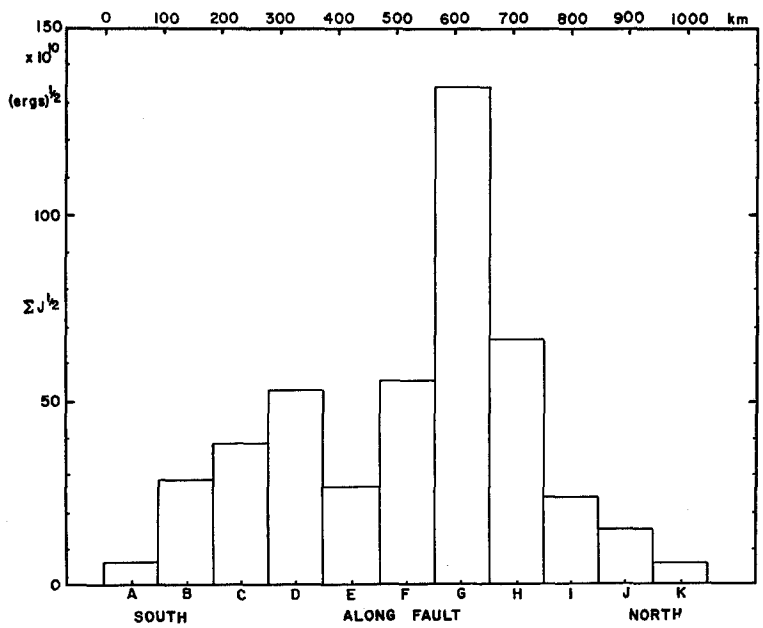

Fig. 2. Distribution of $\Sigma J^{\frac{1}{2}}$ along fault in the aftershock area. The letters A, B, C, etc., refer to figure 1.

shock strain release extended substantially from the principal epicenter in both directions along the fault and that it tapered off toward the ends—more rapidly northward than in the reverse direction. It appears therefore that, in the Kamchatka earthquake, faulting was initiated at a point not very far from the middle of the active segment, whereas in the Kern County earthquake (Benioff, 1955*a*) it began at one end of the segment. Moreover, in the Kern County earthquake the aftershock strain release was greatest at the two ends of the active segment, whereas in the Kamchatka shock it was greatest near the middle.

For shocks for which epicenters were not given, the differences in arrival times of P at several stations were used. This permitted a definite decision as to whether or not a given shock should be included.

b) Depth distribution.—Shocks with focal depths in excess of 150 km. are excluded from our lists. Only a small number of the shocks used occurred at depths between 60 and 150 km. On the other hand, the majority of the earthquakes exhibited clear second phases, pP, usually 9 to 13 seconds after P. Assuming that the focus is situated at the Mohorovičić boundary, the crustal thickness h is related with sufficient accuracy to the time difference between P and pP by the formula

$$h = \frac{(T_{pP} - T_P)v_1}{2\left[1 - \left(\frac{v_1}{R}\frac{dT}{d\Delta}\right)^2\right]^{\frac{1}{2}}} \tag{11}$$

where v_1 = the mean velocity for P waves in the crust,
R = the earth's radius,
Δ = the epicentral distance.

For $\Delta = 60°$ (mean distance to Uppsala and Kiruna) and $v_1 = 6.3$ km/sec., we find

$$h = 3.40\,(T_{pP} - T_P)\text{ km.} \tag{12}$$

when the time difference is expressed in seconds. The following numerical values are obtained:

$T_{pP} - T_P$ (sec.)	h (km.)
9	31
10	34
11	37
12	41
13	44

Since the depth of the Mohorovičić discontinuity very likely lies within this range, we may assume that the foci of the majority of the aftershocks in our list were situated in or near the discontinuity. Monakhov and Tarakanov (1955) found an average depth of 60 km. from observations at near-by stations.

c) Magnitude limit.—In constructing a strain release curve the magnitude limit should be chosen as low as the completeness of the data will permit. We assume that the distribution of aftershocks in respect to magnitude is such that omission of shocks below our lower magnitude limit does not substantially alter the strain-

release characteristic except as to absolute values. The inclusion of an incomplete number of shocks of lower magnitude would introduce substantial errors in the method.

The relation of the rate of strain release in an aftershock sequence to the magnitude M can be calculated as follows. Let

N = the number of shocks of magnitude M occurring in unit time interval within the area considered,

M_0 = the magnitude of the largest shock in the aftershock sequence,

M_1 = the lower magnitude limit, chosen such that the material is homogeneous for $M \geqq M_1$,

a, b, α, β = constants,

S = $\Sigma J^{\frac{1}{2}}$ introduced for convenience,

S' = dS/dt,

q = $\log_{10} e$.

We have the following relations

$$\log J^{\frac{1}{2}} = a + bM \tag{13}$$

$$\log N = \alpha - \beta M \tag{14}$$

and

$$S' = \int_{M_1}^{M_0} N\, J^{\frac{1}{2}}\, dM \tag{15}$$

Carrying out the integration we find

$$S' = \frac{q10^{\alpha+a}}{b-\beta}\left(\exp\left[\frac{b-\beta}{q} M_0\right] - \exp\left[\frac{b-\beta}{q} M_1\right]\right) \tag{16}$$

This gives

$$\frac{dS'}{dM_1} = -10^{(\alpha+a)+(b-\beta)M_1} < 0\ ,$$

i.e., the higher we choose the magnitude limit, the lower is the rate of strain release. It is important always to consider that S' depends upon M_1. For a given series, i.e., a given M_0 and given α and β, we can reduce one rate S_1' referred to M_1 to another rate S_2' referred to another magnitude limit M_2 by the following formula:

$$\frac{S_2'}{S_1'} = \frac{1 - \exp\left[\frac{b-\beta}{q}(M_2 - M_0)\right]}{1 - \exp\left[\frac{b-\beta}{q}(M_1 - M_0)\right]} \tag{17}$$

In comparing two different series having different M_0, α, and β, we reduce S' for the series with the largest M_1 to the value corresponding to the lower M_1.

In our case we have used $\beta = 0.9$ (Gutenberg and Richter, 1954). In this case we find

$$S' = 10^{\alpha+a}(M_0 - M_1) \tag{18}$$

The reduction from S_1' (corresponding to M_1) to S_2' (corresponding to M_2) can then be performed for a given series by means of the relation

$$\frac{S_2'}{S_1'} = \frac{M_0 - M_2}{M_0 - M_1} \tag{19}$$

This formula has been well confirmed in a comparison of the strain-rebound characteristics of all world shallow earthquakes of magnitudes $\geqq 8.0$ with that for magnitudes $\geqq 7\frac{3}{4}$ (Benioff, 1951*b*, figs. 1 and 5, resp.). In this example the left-hand side of equation (19) is 0.68, and the right-hand side is 0.71.

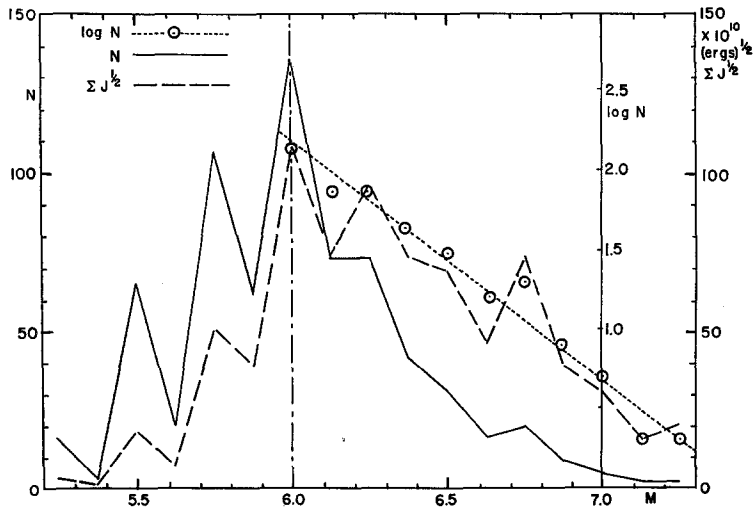

Fig. 3. $\Sigma J^{\frac{1}{2}}$, N (number of shocks), and log N plotted against magnitude M for the aftershocks. The scales of N and log N are independent of each other in the graph.

The value $\beta = 0.9$ derived for independent earthquakes has also been found to apply to most aftershock sequences. However, in the Kamchatka sequence β is equal to 1.5, as may be seen in figure 3. Plotting $\Sigma J^{\frac{1}{2}}$ and the number N of shocks against M (fig. 3) we find that our lower magnitude limit is 6.0. For $M \geqq 6.0$ the number N shows the typical exponential decrease with increasing M, but not for lower values of M. Therefore only shocks with $M \geqq 6.0$ are used in constructing the strain release.

d) Secondary aftershocks.—Several of the larger aftershocks have their own series of aftershocks, which may be considered secondary aftershocks in the main series. Such aftershocks were included since frequently it would have been completely arbitrary or impossible to distinguish between primary and secondary aftershocks. In any case, the larger aftershocks, which dominate the strain-release curve, are primary.

We have used a total of 409 earthquakes. An additional 373 shocks were listed in the bulletins of Kiruna and Uppsala with magnitudes in the range 5–6. Many more were recorded with smaller magnitudes.

2. Strain Release in the Aftershock Sequence

In figure 4, $\Sigma J^{\frac{1}{2}}$ is plotted against log t, t being the time in days counted from the time of origin of the main shock. The straight lines in figure 4 indicate the mean rate of strain release. They have been drawn slightly to the left of the plotted points, so as not to interfere with them. The characteristic shows three main segments, each of which can be represented by an equation of the form

$$\Sigma J^{\frac{1}{2}} = A + B \log t, \tag{20}$$

A and B being constants. The breaks in the curve occur at $t = 0.4$ days and $t = 195$ days, the latter being particularly pronounced. The following values of B are obtained from the curve:

t	B
0–0.4 days	62.68×10^{10} (ergs)$^{\frac{1}{2}}$
0.4–195	123.39
>195	308.13

It is a remarkable fact that these values of B have almost the exact ratios of 1 : 2 : 5. The probability that these ratios represent pure chance seems quite small. However, the explanation is by no means clear. For the Signal Hill aftershock series (Benioff, 1951*a*) the ratio of the coefficients B was 1 : 2.14 or very nearly 1 : 2.

With the help of the formulas developed in section 1, above, we are able to compare some of the aftershock sequences studied earlier. Using the same units as the foregoing, Benioff (1951*a*) found the following values of B in the equation $\Sigma J^{\frac{1}{2}} = A + B \log t$:

	B (Benioff, 1951*a*)	Corresponding magnitude range	B reduced to $M_1 = 3.0$
Manix	6.	3.0–5.1	6.4
Long Beach	18.2	3.9–5.4	29.1
Nevada	34	3.3–5.9	38
Hawke's Bay	27	4.1–6.9	38

It is interesting to note that the values of B, reduced to a common magnitude limit of 3.0, are the same for Nevada and Hawke's Bay. Reducing the strain-release curve for the Kern County aftershocks (Benioff, 1955*a*, *b*) to the same a as for the shocks above, i.e., $a = 6$ instead of 4.5, and to $M_1 = 3.0$, we find B for the first segment (S_a) to be 45.

The first listed aftershock in the Kamchatka sequence occurred at $t = 0.06$ days. No shocks could be distinguished earlier, owing to masking of the records by the large shock. The shock which initiated the third phase at 195 days had a magnitude between 6¾ and 7, and it was the largest in the 133-day interval following the shock at $t = 61.7$ days.

The Kamchatka strain-release characteristic belongs to the class in which the strain release is represented by the single equation $\Sigma J^{\frac{1}{2}} = A + B \log t$. It differs from characteristics studied earlier in having three segments.

With a length of 1,030 km. and a width of 240 km., the aftershock area amounts to 2.47×10^{15} cm.^{2}. We assume that the average depth of the strain region is 60 km., since the foci of many aftershocks were found down to this depth. The total volume

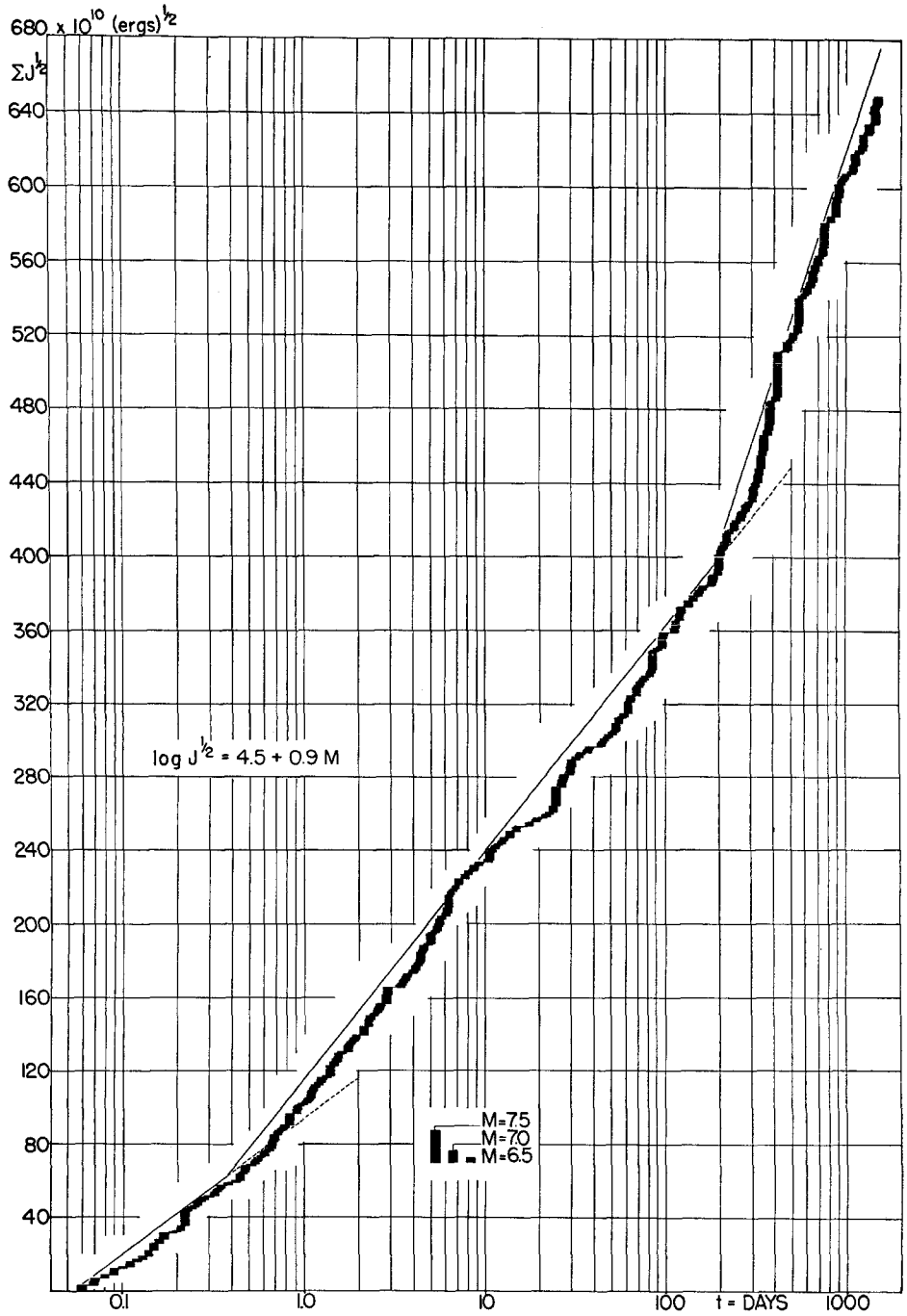

Fig. 4. Strain-release characteristic for the aftershock sequence for all shocks with $M \geqq 6.0$.

of the strained rocks is $V = 1.483 \times 10^{22}$ cm.^{3}. The seismic-wave energy of the principal shock is $J = 2 \times 10^{24}$ ergs. This gives us an average elastic energy density of 1.35×10^2 ergs/cm.^{3}. From formula (4) of section 1, i.e.,

$$\epsilon^2 = \frac{2j}{\bar{\mu} V}$$

assuming $p = 1$ and putting $\bar{\mu} = 6 \times 10^{11}$ dynes/cm.^{2}, we find $\epsilon^2 = 4.5 \times 10^{-10}$. The elastic strain preceding the principal earthquake is thus $\epsilon = 2.1 \times 10^{-5}$. The total strain release in the aftershocks up to the beginning of December, 1956, for $M \geqq 6.0$ is proportional to $\Sigma J^{\frac{1}{2}} = 650 \times 10^{10}$ (ergs)$^{\frac{1}{2}} = 6.5 \times 10^{12}$ (ergs)$^{\frac{1}{2}}$. For the principal earthquake the corresponding quantity is $J^{\frac{1}{2}} = 1.41 \times 10^{12}$ (ergs)$^{\frac{1}{2}}$. Since the aftershock sequence is not yet terminated, the elastic creep strain is more than 4.6 times as large as the purely elastic strain, assuming the creep elastic constant to be equal to $\bar{\mu}$ and the same volume V to be involved in both cases. The total average strain just preceding the big earthquake is $\epsilon = 11.9 \times 10^{-5}$.

The elastic stress just before fracture is roughly $\sigma = \epsilon\bar{\mu} = 2.1 \times 10^{-5} \times 6 \times 10^{11} = 1.26 \times 10^7$ dynes/cm.^{2} = 12.6 kg/cm.^{2} If W = the width of the aftershock region, the total relative slip y during the principal shock is $y = \epsilon W = 2.1 \times 10^{-5} \times 2.4 \times 10^7$ cm. $= 5.0 \times 10^2$ cm. = 5.0 meters. This is naturally a rough approximation, since ϵ as used here represents the shear strain only very approximately, but appears reasonable in view of displacements observed in other great shocks such as San Francisco, 1906 ($M = 8\frac{1}{4}$).

3. North Japan–Kamchatka Regional Strain-Release Characteristics

In an aftershock sequence such as this it is difficult to determine the termination of the series. As a way out we propose to compute the strain release for the entire north Japan–Kamchatka region over the past half century and from this to determine the rate for the portion of the area represented by the Kamchatka, 1952, strain zone. We assume that the aftershock sequence terminates when its rate of strain release per unit area becomes equal to that of the secular rate per unit area, determined for the region as a whole.

The secular strain release characteristics of the whole system for shallow shocks ($h \leqq 60$ km.) and for shallow plus intermediate shocks are shown in figure 5 for the interval 1897–1956. The data for these curves were taken from Gutenberg and Richter (1954), supplemented by unpublished revisions of magnitudes supplied by Dr. Gutenberg; further from Gutenberg (1956); and a few independent computations taken from the Kamchatka sequence. In view of the limited time in which observations of earthquakes are available we feel that the specific strain rate of the entire region is more nearly indicative of the actual value than could be determined from the aftershock area only. We have taken magnitude $7\frac{1}{4}$ as the lower limit for the secular curves in order that each series be complete.

It is clear from figure 5 that the shallow activity of this region has not proceeded at a uniform rate, but rather in steps corresponding closely though not exactly with the behavior of the world shallow strain-release characteristic (Benioff, 1951*b*). It is interesting to note that on March 4, 1952, the great Japanese earthquake of magnitude 8.6 occurred in the southern part of the region represented by the curves of figure 5. The dashed curves were drawn to indicate the mean characteristics.

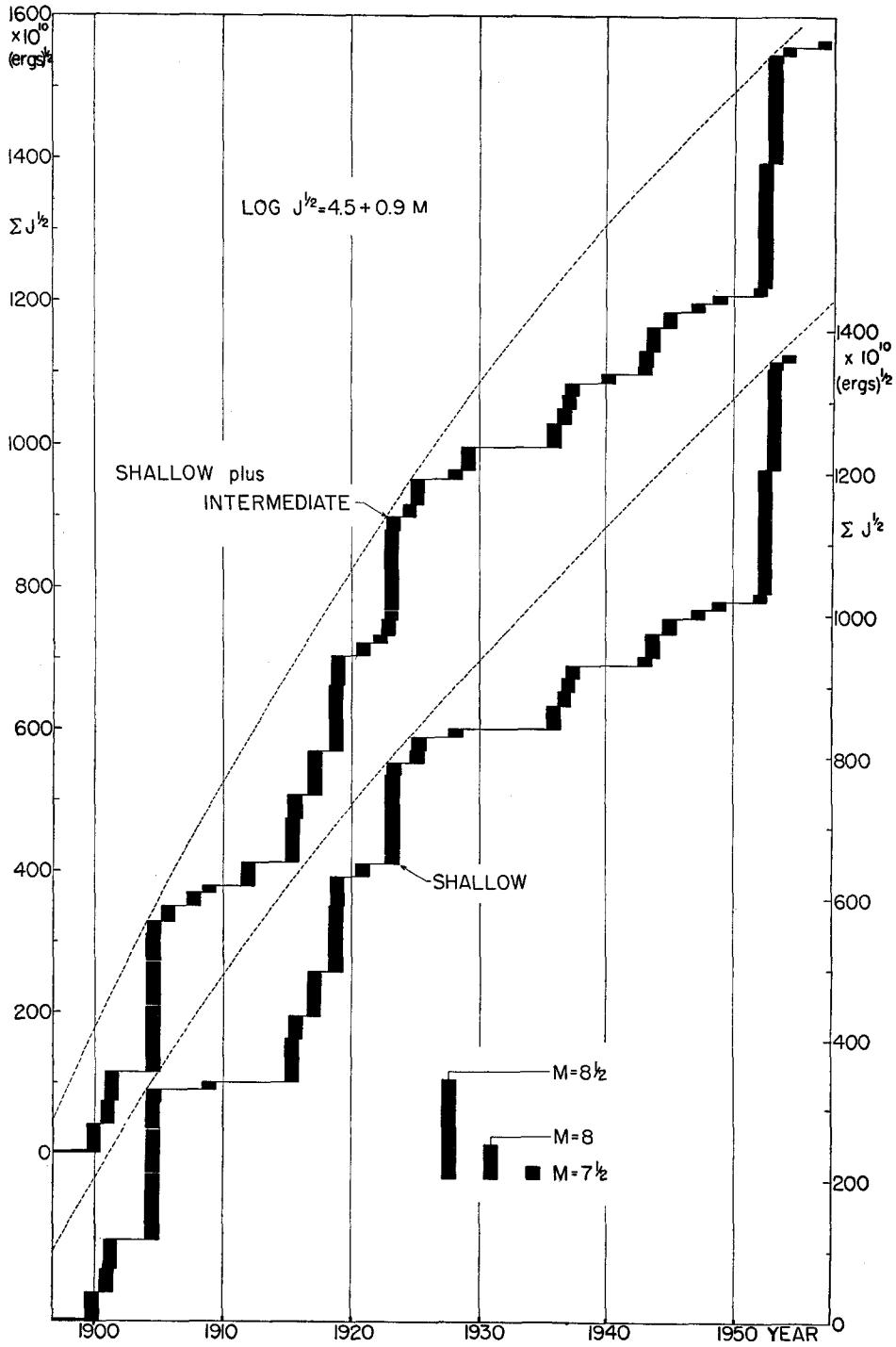

Fig. 5. Strain accumulation and release for the stress system Kamchatka–Kurile Islands–north Japan for all shocks with $M \geqq 7\frac{1}{4}$.

Figure 7 shows the total regional strain release from 1897 to 1956 as a function of distance along the arc for each of the sections 1 to 7 shown in figure 6.

Referring to the curves in figure 5, the current rate of secular strain relief is 0.049×10^{10} (ergs)$^{\frac{1}{2}}$/day, and the ratio of the aftershock area to that of the whole region is 0.6. Using equation (19) the regional secular rate can be calculated for a lower magnitude limit $M_1 = 6$ by multiplying by 1.9. Hence the duration of the aftershock sequence in days is computed from the following equation:

$$\frac{308}{t} = 0.049 \times 1.9 \times 0.6$$

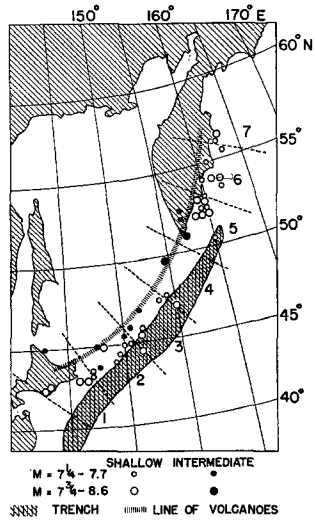

Fig. 6. Map showing the locations of all shocks used in constructing the strain relief curves in figure 5. Other shocks are not shown in this map.

Thus if it continues at its present rate the aftershock strain rate becomes equal to the reduced regional secular strain rate at $t = 15$ years after the origin time of the principal shock. This is a very rough approximation, since it also depends upon constancy of the assumed regional rate.

4. Aftershock Mechanism

The abrupt discontinuities in rate of strain release in the aftershock sequence at $t = 0.4$ and $t = 195$ days must represent some fundamental change in the system. An examination of the geographic and depth distributions of the foci shows random characteristics both before and after the times of the discontinuities. We conclude therefore that the discontinuities must be due to changes in mechanism.

We assume that the strike of the fault corresponds with the long direction of the aftershock area. The active segment was parallel to the strike of the oceanic deep and the line of volcanoes. Hodgson (1956) gives two possible solutions for the fault-slip direction derived from observations of the first motion of longitudinal waves. The one having a strike of N 10° E and a dip of 79° with dextral slip must therefore be the correct solution. On the other hand, he assumes that the principal earthquake was in fact two shocks, the second occurring 10 seconds after the first. We are of

the opinion that the principal earthquake was single rather than double, for the following reasons:

a) The second phase, which he interprets as the P phase of a second earthquake, occurs 10 seconds after the original P. This time interval corresponds very nearly with the average pP − P interval exhibited by earthquakes of the aftershock series. It is very difficult for us to understand how the principal earthquake can be interpreted as two shocks without at the same time assuming that each of the aftershocks is also two earthquakes. Hutchinson (1954) assumes a single shock and interprets the second phase as pP.

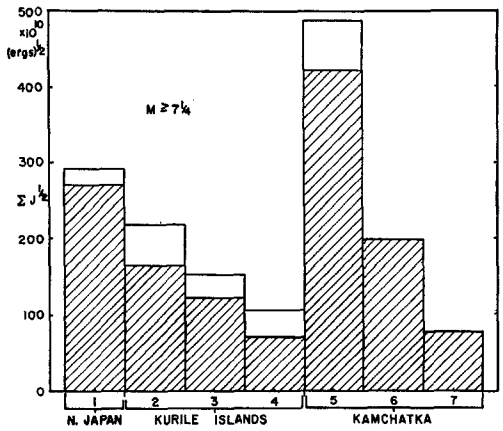

Fig. 7. $\Sigma J^{\frac{1}{2}}$ plotted along the axis Kamchatka–north Japan. The numerals 1, 2, 3, etc., refer to those of figure 6. Dashed blocks refer to shallow shocks only. The total $\Sigma J^{\frac{1}{2}}$ for any section includes both shallow and intermediate shocks.

b) With the interpretation of dual shocks Hodgson's (1956) solutions required the second earthquake to be generated by movements approximately opposite in direction from those of the first. For an earthquake of Kamchatka's magnitude such reversals of movement are extremely unlikely.

c) Hodgson (1956) bases part of his argument for a dual origin on the observation that the time interval between the first two phases is essentially constant for all stations. However, since within the limit of observational errors the difference pP − P is also independent of the coördinates of the stations, there is no compelling reason for assuming a dual source.

Hodgson (1956) has collected data on the observed initial motions at numerous stations for a number of the larger aftershocks. For approximately half of these he was able to find a fault-plane solution. There were five shocks, however, for which he was unable to find a solution. Fortunately, he included the observational data for these anomalous shocks also. These observations of direction of first motions are all plotted on a single graph shown in figure 8. This graph represents a horizontal plane through the focus, with station azimuth and the angle which the departing ray makes with the earth's radius (angle of incidence) as polar coördinates. This graph provides a clear and direct representation of the radial motion at the source responsible for the observed first motion at any given station and does not depend upon any assumption concerning the type of movements generated at the source.

Båth (1957) has developed formulas and figures illustrating the first-motion patterns characteristic of different types of fault movements. The only pattern generated by a simple fault which at all resembles the observed pattern is that of case 2c (*loc. cit.*), if the directions of motion are reversed in this case. Here, however, the fraction of

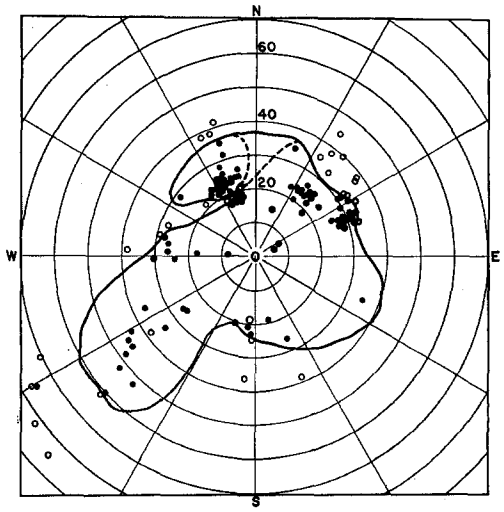

Fig. 8. Graph of observed polar distribution in lower half space of dilatations (open circles) and compressions (dots) for five anomalous shocks in the aftershock area. Coördinates are station azimuth and angle of incidence at the focus O.

the area of the half sphere occupied by compressions is 0.50, whereas in the observed distribution (fig. 8) the corresponding fraction is 0.18. It is clear that no simple fault source can satisfy the observed pattern. This pattern can be interpreted as generated by a graben source.

A most remarkable feature of these graben type aftershocks is that they occur only in the third phase of the strain-release curve and in a limited region near the western side of the central aftershock area. These clearly represent a different mechanism from that of the majority of the aftershocks which continues to operate also.

References

BÅTH, M.

1957. "Polar Graphs of Initial Motions at an Earthquake Source," *Bull. Seism. Soc. Am.* (in press).

BENIOFF, H.

1951*a*. "Earthquakes and Rock Creep," *Bull. Seism. Soc. Am.*, Vol. 41, No. 1, pp. 31–62.

1951*b*. "Global Strain Accumulation and Release as Revealed by Great Earthquakes," *Bull. Geol. Soc. Am.*, Vol. 62, pp. 331–338.

1955*a*. "Seismic Evidence for Crustal Structure and Tectonic Activity," Geol. Soc. Am., *Spec. Paper* 62, pp. 61–73.

1955*b*. "Mechanism and Strain Characteristics of the White Wolf Fault as Indicated by the Aftershock Sequence," California Division of Mines, *Bull.* 171, pp. 199–202.

BULLEN, K. E.

1947. *An Introduction to the Theory of Seismology*, Cambridge Univ. Press, 276 pp.

GUTENBERG, B.

1956. "Great Earthquakes, 1896–1903," *Trans. Am. Geophys. Union*, Vol. 37, No. 5, pp. 608–614.

GUTENBERG, B., and C. F. RICHTER

1954. *Seismicity of the Earth*, Princeton Univ. Press, 310 pp.

1956. "Magnitude and Energy of Earthquakes," *Ann. di Geofisica*, Vol. IX, No. 1, pp. 1–15.

HODGSON, J. H.

1956. "Direction of Faulting in Some of the Larger Earthquakes of the North Pacific, 1950–1953," *Publ. Dom. Obs. Ottawa*, Vol. XVIII, No. 10, pp. 219–252.

HUTCHINSON, R. O.

1954. "The Kamchatka Earthquakes of November, 1952," *Earthq. Notes*, Vol. XXV, Nos. 3–4, pp. 37–41.

MONAKHOV, F. I., and R. Z. TARAKANOV

1955. "Characteristics of Earthquakes in the Kurile Islands and Kamchatka according to Observations of Near Stations in the Years 1952–1954" [in Russian], *Izvest. Akad. Nauk SSSR*, Ser. Geofiz., No. 5, pp. 401–415.

SEISMOLOGICAL LABORATORY,
CALIFORNIA INSTITUTE OF TECHNOLOGY,
PASADENA, CALIFORNIA.
(Division of Geological Sciences, contribution no. 824.)